Experimental study of the interaction of subpicosecond laser pulses with solid targets of varying initial scale lengths

S. Bastiani,[1] A. Rousse,[2] J. P. Geindre,[1] P. Audebert,[1] C. Quoix,[2] G. Hamoniaux,[2] A. Antonetti,[2] and J. -C. Gauthier[1]
[1]*Laboratoire pour l'Utilisation des Lasers Intenses, UMR 100 du Centre National de la Recherche Scientifique, Ecole Polytechnique, 91128 Palaiseau, France*
[2]*Laboratoire d'Optique Appliquée, URA 1406 du Centre National de la Recherche Scientifique, Batterie de l'Yvette, 91761 Palaiseau, France*
(Received 13 June 1997)

We have studied experimentally the angular and energy distribution of the suprathermal electrons produced during the interaction of a 120 fs, 50 mJ, 800 nm, *P*-polarized laser pulse on SiO_2 targets. A sharply collimated jet of electrons is observed in the laser specular reflection direction, in the plane of incidence, superimposed to an angularly uniform electron distribution. Electron energies are $\approx$20 keV for a laser intensity of 4×10^{16} W cm^{-2} and 45° incidence angle. The electron jet is weaker and angularly broadened with the introduction of a laser prepulse controlling the electron density gradient scale length. Laser absorption and $K\alpha$ line intensity measurements show a maximum for a prepulse delay of $\approx$6 ps with an electron energy rising to $\approx$180 keV. Gradient scale length measurements at this prepulse delay fit the laser absorption peak scaling obtained from standard resonant absorption theory. [S1063-651X(97)07612-5]

PACS number(s): 52.50.Jm, 52.40.−w, 52.70.Kz, 52.40.Nk

I. INTRODUCTION

The recent advent of compact high-intensity subpicosecond lasers with chirped pulse amplification (CPA) [1] has opened a new field of study of laser matter interaction with solid targets [2–4]. One of the most important features of this new approach is the study of laser-produced plasmas on a new time scale for which, in principle, hydrodynamic motion is no longer a dominating factor. This enables the production of plasmas at high electron energy density with highly transient and nonequilibrium states resulting from the very short temporal (<ps) and spatial (<100 nm) scales involved. Recently, these plasmas have attracted attention as potential sources for ultrafast pulsed x rays in the sub-keV energy range [5–7], the keV range [8–10], and the MeV range [11]. Vigorous experimental efforts for bringing picosecond time resolution in diffraction, spectroscopy, or microscopy of transient physical [12], chemical [13], or biological phenomena [14] have started.

Over the last few years it has been recognized in several fields of laser plasma interactions that the temporal shape and the intensity contrast ratio of the laser pulse are of paramount importance in tailoring the plasma properties. For example, the importance of a controlled prepulse (or multipulses) in the pumping and amplification of x-ray lasers has been reviewed recently [15]. Another example is the enhancement of water-window x-ray emission from laser-irradiated liquid droplets by a low-energy UV prepulse [16]. In short-pulse high-intensity laser interactions, it has been early recognized that the x-ray yield is increased if the laser interacts not with the surface of the solid material but with a preformed plasma originating from irradiation of the solid surface with an earlier pulse or with amplified spontaneous emission (ASE) from the laser [17–19]. Recent systematic experiments have demonstrated that the presence of a weak prepulse boosts the x-ray conversion efficiency from solid target laser-produced plasmas [20–23]. Ironically, a plasma can also play a role in prepulse suppression to generate clean, high-intensity subpicosecond laser pulses through self-induced plasma-shuttering effects [24,25].

By varying the temporal separation between the main laser pulse and a prepulse, one can generate preformed plasmas with different scale lengths and density gradients. We define the electron density gradient scale length as the inverse of the logarithmic derivative $[(1/n_e)(dn_e/dx)]^{-1}$. The description of the numerous linear and nonlinear laser absorption mechanisms in the ultrashort laser pulse regime for different values of L/λ (where λ is the laser wavelength) is far outside the scope of this experimental paper. A comprehensive review of state-of-the-art theory has been given recently [4]. Here, we restrict ourselves to summarizing the basic features of laser absorption in the $0<L/\lambda<1$ reduced scale length range.

First, it is important to note the strong influence of the laser incidence angle and polarization state in short-pulse laser interactions because many of the basic plasma properties are controlled by the strong laser field rather than by its own density and temperature. This is particularly true for *P*-polarized (TM) laser light and oblique incidence because resonance absorption [26] is a very efficient absorption mechanism for finite reduced scale length plasmas. For reduced scale lengths $L/\lambda\ll1$, the laser interacts with a steplike density profile. Under these conditions, the interaction takes place in the skin layer of an overdense plasma ($n_e\gg n_c$) where n_c is the critical density at laser wavelength λ. At laser intensities below 10^{16} W cm^{-2} electron temperatures are in the sub-keV range and the main laser absorption mechanism is related to electron collisions in the skin layer [27,28]. At higher laser intensities, the electron mean free path exceeds the skin depth leading to the anomalous skin effect and collisionless energy absorption. The intensity separation of these two absorption mechanisms has been

clearly established [27,29]. As hinted at earlier, resonant absorption is another absorption mechanism although it is not clear how effective this is in steplike density gradients. In the limit of high intensities—when the electron excursion in the laser field is larger than the gradient scale length $L/\lambda < (2\pi)^{-1} v_{osc}/c$ (where $v_{osc} = eE_0/m\omega$ is the quiver velocity)—electrons are directly heated by the P-polarized component of the laser field (vacuum heating) [30,31]. This absorption mechanism is important when the light pressure (associated to the ponderomotive force) is greater than the plasma pressure. For larger values of L/λ, resonant absorption has been shown to play a major role in laser absorption [28,32–34] for P-polarized light.

Experimental studies of short-pulse laser interactions have used a number of ''observables'' as a signature of laser absorption mechanisms. Among these, direct optical measurements of the reflectivity [35] and absorption [36] have brought some understanding of the physical situation for collisional absorption mechanisms. X-ray spectroscopy of highly charged ions [8,37] has been used as a powerful diagnostic tool of the plasma parameters. Suprathermal (''hot'') electron generation by nonlinear (collisionless) processes [38] has been studied by $K\alpha$ line radiation produced by knocking out a bound K-shell electron from witness layers buried at various depths in the bulk of the target [9,39], by fast-ion blow-off detection [40,41], and by simultaneous measurements of x rays, electrons, and far infrared (FIR) radiation [42].

Most of the previous characterizations of hot electron energies have been made for the electron population which penetrates into the cold region of the target beyond the heat front [9,39]. Hot electrons created with initial velocities outwards of the target surface are strongly repelled towards the target's bulk by the charge separation field generated by the less mobile ions. However, very few detailed experimental studies have been performed on the population of electrons which have sufficient energy to overcome the barrier set up by the charge separation potential and which escape freely into the vacuum. In nanosecond pulse interactions performed at a 0.26 μm laser wavelength [43], an angular distribution strongly peaked along the laser axis has been exhibited for the more energetic electrons. Recently, highly peaked MeV electrons have been observed [44,45] at relativistic laser intensities where v_{osc} exceeds the speed of light in vacuum.

Here, we present experimental results of the angular distribution and energy spectrum of hot electrons produced during the interaction of a P-polarized, 4×10^{16} W cm^{-2} intensity, 45° angle of incidence, laser pulse of 120 fs duration on fused silica targets. We change the electron density gradient scale length by varying the temporal separation between the main laser pulse and a prepulse of the same duration but with 1% of the intensity of the main interacting pulse. Doing this, we explore the highly complex transition between steplike gradient absorption and resonant absorption. The electron density gradient scale length produced by the earlier pulse is measured as a function of time by dual-polarization frequency domain interferometry [46–49]. These measurements are correlated with Si $K\alpha$ line emission from the bulk of the target. We find an optimum delay between the prepulse and the main pulse for which the laser absorption and the $K\alpha$ yield are greatly enhanced with respect to prepulse-free conditions. With prepulse-free irradiation, highly collimated electron jets have been observed in the direction of the specularly reflected laser light.

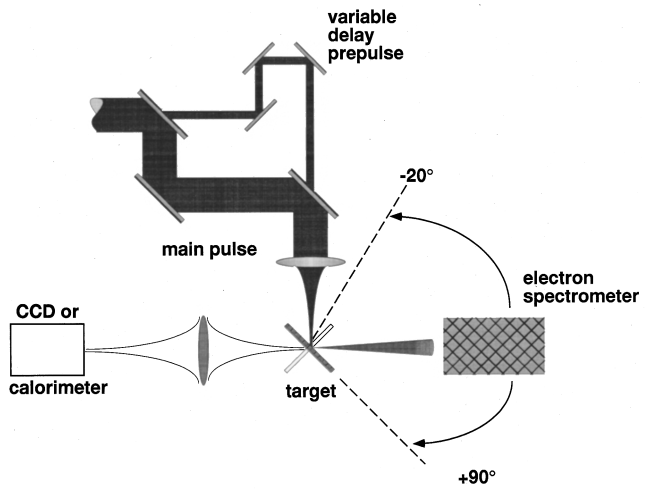

FIG. 1. Schematic experimental apparatus showing the pulse-prepulse optics, the angle-resolving electron spectrometer, and the specularly reflected laser optical diagnostics.

II. EXPERIMENTAL SETUP

The experiments were carried out with the Laboratoire d'Optique Appliquée Ti:Al_2O_3 CPA laser in Palaiseau [50]. This laser is capable of delivering 120 fs duration, 60 mJ energy, 800 nm wavelength, 10 Hz repetition rate pulses. The laser was equipped with a specially designed doublet stretcher [51] to compensate for phase errors of third and fourth order. With this important addition, the laser intensity contrast ratio was measured to be better than 10^{-8} (at 2 ps before the main pulse) by high-dynamics third order autocorrelation techniques. The main laser pulse was focused onto the target at various incidence angles by a 40 cm (f/16) focal length MgF_2 lens on solid SiO_2 flat targets.

In Fig. 1 is sketched the experimental setup and, in particular, the arrangement utilized for the controlled prepulse production. The 20 mm diameter [full width at half maximum] (FWHM) main laser beam is reflected on a mirror having a 6 mm diameter hole drilled in its center that allows the transmission of a small part of the beam profile. This beam is time delayed with a variable delay line and, after transmission through a second apertured mirror, is superimposed to the main laser beam. Typically, this system gives intensities on the target of 4×10^{16} W cm^{-2} for the main pulse and 4×10^{14} W cm^{-2} for the prepulse. A diffraction-limited focal spot of 140 μm diameter for the prepulse and a slightly elliptical 32×18 μm^2 for the main pulse were obtained at $1/e^2$ of maximum intensity. Targets were mounted on an X-Y-Z motorized translational system to expose a fresh surface of the target to each laser shot.

The diagnostic of the suprathermal electrons is a multichannel electron spectrometer, fitted with a permanent magnetic field of $\approx$260 G. The detectors are six silicon surface barrier detectors, with an active thickness variable between 100 and 1000 μm. The energy range covered by this instrument extends from 20 to 200 keV. The lower end of this

energy range is higher than the low-energy cutoff for electrons to escape the plasma which can be estimated from the potential related to the ponderomotive force of the incident laser pulse or from the electrostatic potential associated to the nonoscillating sheath electric field [29] to be ≈ 5 keV in our conditions. The spectrometer can be rotated, in 1° steps, around a vertical axis passing through the plasma, in order to investigate the angular distribution of the emitted electrons in the incidence plane. It can also be positioned out of this plane, to investigate the electron emission in the azimuthal direction. This allows us to get an insight into the whole 2π sr angular electron distribution. Each photodiode is filtered with a 1.6 μm thick aluminum foil, to protect the diodes against visible light. Contrary to the common practice, we have not placed the filter directly over the entrance slit of the spectrometer in order to minimize electron scattering in the spectrometer. To make sure that the signal is actually due to electrons, we made null tests (i) by closing the spectrometer with a 2 mm thick glass plate to stop all the electrons and UV and soft-x-ray radiation and (ii) by adding, near the target front face, another magnetic field to deflect the electrons. Both tests give null signals, allowing us to measure the diode noise level with the laser switched on. The collection angle of the electron spectrometer was of the order of 8×10^{-4} sr. Systematic errors, mainly due to the calibration of the detection system, on the absolute number of electrons is of the order of 50%.

The plasma reflectivity measurements have been performed by means of a calorimeter (see Fig. 1). A slight focusing (with an $f/8$ lens) of the reflected beam ensured that the whole beam was collected by the calorimeter. Near-field images of the reflected pump beam were also obtained by a charge-coupled device (CCD) camera. For the electron density gradient scale length measurements [49], we used the technique of frequency-domain interferometry that we have extended to allow simultaneous measurements of the phase shift for the two (S and P) probe polarizations. Details on this technique are given elsewhere [46,47].

The Si $K\alpha$ emission was dispersed by means of a Von Hamos spectrograph built with a PET (pentaerythritol) crystal ($2d=8.742$ Å) having a 10 cm curvature radius. The spectra were collected at an angle of 10° with respect to the target normal with a cooled (-40 °C) x-ray sensitive CCD camera [9]. To decrease the background of the CCD image (which was attributed to high-energy electron-induced x-ray fluorescence from the crystal) the entire interaction region was shielded with a lead enclosure.

III. EXPERIMENTAL RESULTS

Experimental results presented here have been obtained for a laser pulse incident on target at an angle of 45° with respect to the normal of the target. As stated earlier, laser intensities were kept constant at 4×10^{16} W cm^{-2} (normal incidence) for the main pulse and at 4×10^{14} W cm^{-2} for the prepulse.

A. Absorption measurements

In Fig. 2 we show the measured reflection coefficient of the main pulse and in Fig. 3 we present the total energy of the electrons emitted in the incidence plane as a function of the prepulse delay. The level of light scattered out of the collecting optics (see Fig. 1) was found to be negligible. The total energy of the electrons was obtained by integrating the signal of the six diodes over the whole range ($-20°$ to $+90°$ with respect to the normal of the target) of angular positions of the electron spectrometer. Without a prepulse, our measured absorption coefficient is in good agreement with previous measurements [33]. In Fig. 2, the presence of a clear maximum of absorption (we assume that $A=1-R$ where A is the absorption coefficient) can be seen for a delay of ≈ 5 ps. This delay, as we will see below, corresponds to a well-defined initial density gradient scale length. For the same delay, we find also a suprathermal electron energy maximum, as we can see in Fig. 3, which corresponds to an optimum conversion of laser energy into suprathermal electron energy. We find a conversion efficiency of laser energy into suprathermal electron energy of $(0.7\pm0.1\%)$ for a prepulse delay of ≈ 5 ps. We note that this value is very much lower than what was measured in similar conditions [9] before, because here we only have access to the highly energetic electrons escaping in the vacuum.

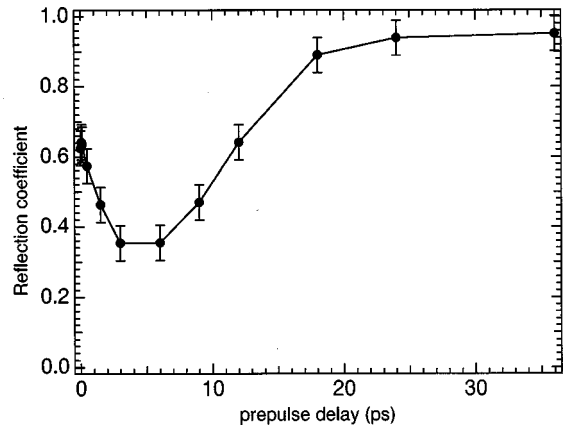

FIG. 2. Reflection coefficient as a function of prepulse delay. The line is an aid to the eye.

Assuming that the predominant absorption mechanism is resonant absorption for scale lengths of the order of a fraction of a laser wavelength (this hypothesis is supported by previous measurements [49] and by theory), one can obtain the condition for optimum absorption using the familiar scaling of peak absorption with the scale length

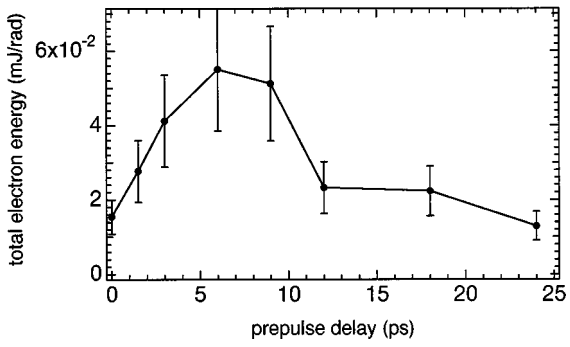

FIG. 3. Total electron energy per unit of solid angle as a function of prepulse delay. The line is an aid to the eye.

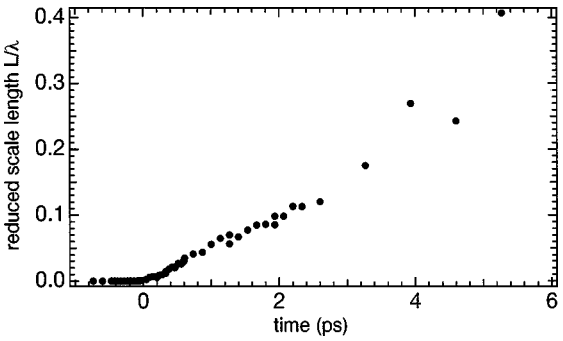

FIG. 4. Reduced electron density gradient scale length as a function of time after the prepulse.

$(2\pi L/\lambda)^{2/3}\sin^2\theta \approx 0.6$ (see Fig. 4 of the Yang *et al.* paper [29]). We obtain $L/\lambda \approx 0.25$. To cross-check this result, we have performed direct measurements of the gradient scale length for laser conditions corresponding to the prepulse target interaction, using the frequency-domain interferometry technique. As noted earlier, we now measure simultaneously the *S*-polarized and *P*-polarized laser probe phase shifts induced by the plasma. This greatly reduces the experimental error on the measurement of the polarization-sensitive phase shift difference because the result is obtained in a single shot. However, we still have to rely on the calculated relation between the (*P*-*S*) phase difference and the plasma scale length (see Fig. 5 of Ref. [49]). For a probe laser incidence angle of 45°, the relative uncertainty on the normalized scale length L/λ for values of ≈ 0.25 is about 30%. This uncertainty is due to the slight variations of the phase shift difference with collisionality and to the neglect of space-time changes of the electron density and temperature gradients in the analysis, as discussed in Ref. [49]. The result of our measurement, reported in Fig. 4, shows that the optimum value of L/λ is reached at a time $t \approx 4.5$ ps, which is consistent with the value obtained for the peak of absorption.

B. Hot electron angular distribution

In Fig. 5, we present the electron angular distribution measured in the incidence plane as a function of the electron spectrometer angle with respect to the normal of the target. Each point in the curve has been obtained by averaging over ten laser shots. These results are obtained with a very steep initial gradient scale length (no prepulse). It shows two remarkable characteristics. First, the absence of a peak of electron emission along the target normal $\theta = 0$, whereas resonant absorption theory foresees an electron acceleration in that direction due to Landau damping or wave breaking of the plasma wave propagating along the electron density gradient. Second, we can see a highly collimated electron emission peak in the specular reflection direction. It is worth noting that this peak contains only 1% of the total number of electrons and that its angular spread is comparable to our stepping angle. The same behavior—a collimated jet of electrons at the specular reflection angle—has been obtained *for all the incidence angles studied* ($20 < \theta < 60°$). However, this effect is more prominent for the incidence angle of 45°.

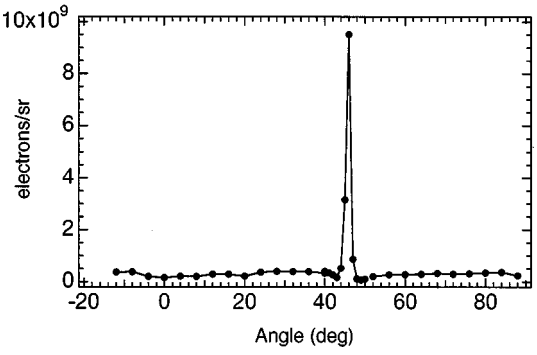

FIG. 5. Angular distribution of suprathermal electrons without prepulse.

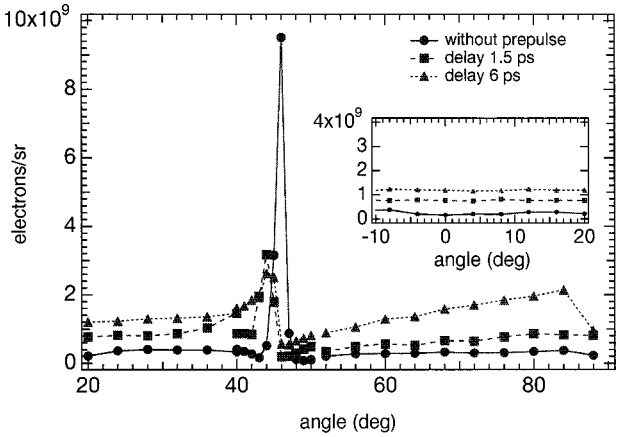

FIG. 6. Angular distribution of suprathermal electrons with prepulse delays of 1.5 and 6 ps. The inset shows the angular region around target normal.

In Fig. 6 we present similar results obtained with two different initial scale lengths *L*: one obtained at the optimum condition for resonant absorption (6 ps delay) and one obtained with a smaller L/λ ($L/\lambda \approx 0.1$), corresponding to a delay of 1.5 ps. The curve obtained with a steplike initial *L* is shown again for comparison. We can immediately see that the angular distribution obtained in the presence of an initial gradient scale length differs from the one obtained with a steplike gradient. In more detail, we can see an important decrease and spread of the emission peak in the specular direction and an increase of the electron emission in the other directions. In addition, we can also note (see the inset in Fig. 6) that there is still no particular electron feature in the direction corresponding to the target normal.

C. Hot electron energy spectrum

We have also analyzed the electron energy spectra, and we have seen that they show large variations depending on the presence (or absence) of an initial gradient scale length. In Fig. 7 we report the spectra, integrated over 10° around the peak emission angle (see Figs. 5 and 6), obtained in the two ''extreme'' interaction conditions: abrupt initial *L* and optimum initial *L* (prepulse delay of ≈ 6 ps) for resonant absorption. Fitted with a Maxwellian distribution over the high-energy region ($E > 30$ keV), we obtain a ''temperature'' of 19 keV in the case of a very steep initial *L* and a ''temperature'' of 182 keV in the other case. We note that the quiver energy of the electrons at our laser intensity is only 3 keV.

Figure 8 shows the temperatures obtained for each emis-

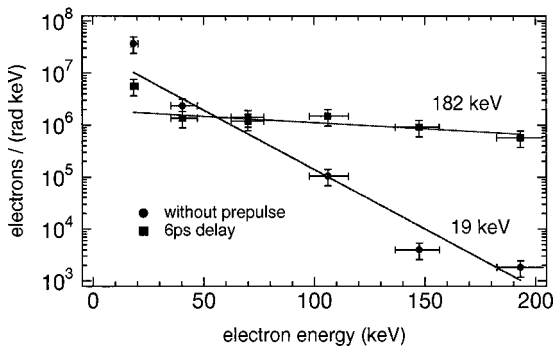

FIG. 7. Electron energy spectra integrated over a 10° interval around 45° observation angle without prepulse and with a prepulse delay of 6 ps. Lines are Maxwellian fits with temperatures of 19 and 182 keV, respectively.

sion angle (averaged over ten laser shots) and for three different initial gradient scale lengths (or prepulse delay). The temperatures obtained in the case of an abrupt initial L show no dependence on the emission angle. On the contrary, with a prepulse, we obtain a maximum in the specular reflection direction. The analysis of the angular distribution of the emission out of the incidence plane (by varying the azimuthal angle of observation of the electron spectrometer) shows that, except for the specular direction, the electron emission is independent of the azimuthal angle. In other words, whatever the azimuthal angle, we obtain an emission identical to the one we get in the incidence plane for observation angles θ outside the interval $40°-50°$. Some of the characteristics of the electron emission, and particularly their isotropic distribution in 2π sr (except in the specular direction), may be explained by the presence of ripples on the plasma surface. In order to verify this hypothesis, we have collected near-field images of the reflected beam on a CCD camera. As stated before, the level of scattered light was very low and we found that the reflected beam was not perturbed by the plasma. We conclude that the plasma surface was very regular, at least on a size scale of the order of λ. Similar results showing the good optical quality of the plasma as a reflector for prepulse suppression have been demonstrated recently [25].

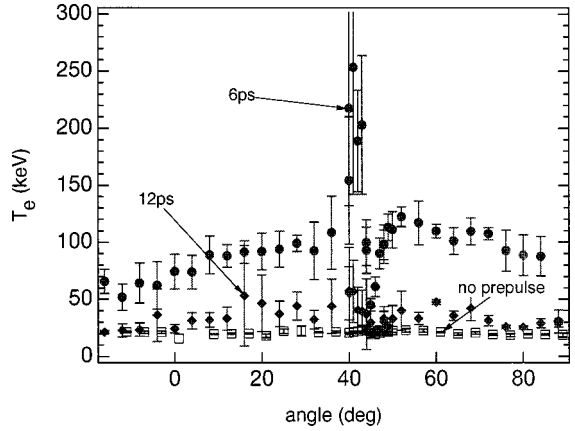

FIG. 8. Hot electron ''temperature'' as a function of laser incidence angle for two prepulse delays. Circles: 6 ps delay; diamonds: 12 ps delay; open squares: no prepulse.

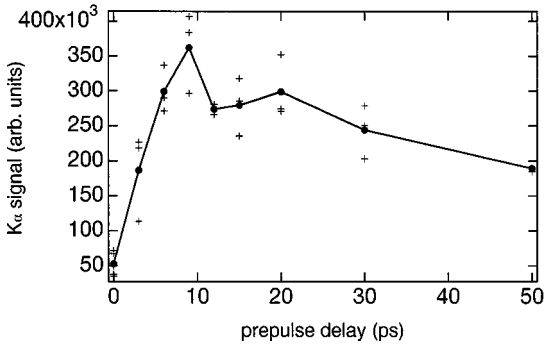

FIG. 9. Si $K\alpha$ emission as a function of the prepulse delay. Dots: average values of individual measurements (crosses). The line is drawn as an aid to the eye.

D. Si $K\alpha$ measurements

$K\alpha$ line emission is generated in the solid material by inner-shell ionization from fast electrons that penetrate in the bulk of the target. Its intensity depends on the electron characteristics: their number and their energy. For light elements like silicon, the K-shell ionization cross section is maximum for electron energies of a few keV, so this line can be used as a diagnostic for ''not-so-hot'' electron production [9]. We have measured the $K\alpha$ emission, again as a function of the prepulse to main pulse delay. The results are shown in Fig. 9, where the crosses are the results of a single measurement and the circles are the averaged values. We observe a strong increase of the $K\alpha$ yield for the first 10 ps and then a slow decrease for longer delays. We obtain an enhancement of about a factor 7 with respect to the case of an abrupt initial gradient for delays corresponding to maximum resonant absorption ($\approx$6 ps). These results show the correlation between the detection of fairly ''hot'' electrons in vacuum by the electron spectrometer and the detection of lower-energy (2–10 keV) electrons by $K\alpha$ line emission. This points to the fact that the electron energy distribution function is highly anisotropic in directions going outwards from and inwards toward the target.

IV. DISCUSSION

In this discussion, we would like to focus on the observed ''jetlike'' electron emission. The shape of the angular distribution of the electrons has no theoretical justification to date. However, the Maxwellian-type energy distribution is supported by particle-in-cell (PIC) [38,52] simulations. Indeed, PIC simulations performed with the EUTERPE code [31] with P-polarized light at 30° incidence angle and 10^{16} W cm^{-2} intensity with mobile ions predict [53] ''hot'' electron temperatures of 20 keV for $L/\lambda = 0.001$ and 170 keV for $L/\lambda = 0.3$, in fair agreement with the observed results. To obtain very high-energy electrons, it is necessary to have first very long acceleration lengths and second very high phase velocity plasma waves. The angular distribution of the electrons is directly related to the plasma wave propagation directions. Recent theoretical results [54,55] and experiments [56] clearly suggesting the possibility of emission of light at the plasma frequency and at its harmonics from the coupling of plasma waves and the laser field in steep density gradients may support the existence of accelerating plasma waves,

even in steplike gradients. Evidence of anisotropic electron energy distributions from Vlasov simulations [57] and kinetic calculations [58–60] has already been presented. However, these distributions have a signature that would pass as electron jets only in the bulk of the target.

One of the most striking observations in these experiments is the sharpness of the collimated electron beam observed in Fig. 5. The jetlike structure could be recorded because of our good angular resolution and fine stepping capability. In addition, this structure was observed only during laser interaction with a steep electron density gradient, i.e., with high contrast ultrashort laser pulses at moderate laser intensities. Returning to Fig. 6, the broadening of the electron peak when a prepulse is applied to the target can be explained by the ''bending'' of the plasma surface. Assuming an exponential electron density gradient, a hypothesis supported by hydrodynamic simulations [61], the location x_c of the critical density n_c can be simply written as a function of the gradient scale length by $x_c = L\ln(n_s/n_c)$ where n_s is the solid density. For the peak absorption scale length, this gives a value of ≈ 1 μm which, when compared to the prepulse focal spot diameter, gives an angular spread of $\approx 3°$, very similar to what we observe. Another interesting feature is the increase of the number of electrons in the grazing direction (parallel to the target) for the prepulse delay of 6 ps. Parametric instabilities such as the ion-acoustic decay in a nonlinearly steepened density profile can produce hot electrons in the transverse direction at the critical density [62]. Excitation of surface waves in a plateau-ramp-type density profile, such as the one produced by laser ponderomotive effects (they are not negligible, even at our moderate laser intensity), also produce ''hot'' electrons in the direction parallel to the surface [63].

V. CONCLUSION

In summary, we have characterized by optical, electron, and x-ray diagnostics the interaction of a subpicosecond, medium-intensity, P-polarized laser with a solid target. By applying a controlled prepulse, we have changed (and measured the change) of the electron density gradient scale length with which the main pulse interacts. Our results exhibit some features that can be explained by standard resonant absorption theory. These are the behavior of the electron number as a function of the incidence angle and the behavior of the reflectivity as a function of the density gradient scale length of the preformed plasma. On the contrary, the presence of an electron emission peak in the specular reflection direction, the absence of any particular electron feature in the target normal direction, and the quasi-isotropic emission in 2π sr over the whole electron energy spectrum are still matters of interpretation. However, it is important to note that the characteristics of these interactions cannot be interpreted on the basis of the presence of ripples on the plasma surface. The important point in our results is the measurement, with such an angular resolution, of the angular and energy distribution of the population of ''hot'' electrons *which escape the plasma* instead of the measurement of the population of electrons which do not overcome the charge separation barrier in front of the target and return to the bulk, as it is usually done in conventional $K\alpha$ studies.

ACKNOWLEDGMENTS

We gratefully acknowledge the support of the laser staff at Laboratory of Applied Optics (LOA) where the experiments were carried out. We would like to thank Jacques Delettrez for his valuable assistance in the use of PIC simulations. The loan of the electron spectrometer from F. Amiranoff is gratefully acknowledged. This work was supported by the Center National de la Recherche Scientifique, the European Community under the Large Facilities Contract No. CHGE-CT93-0021, and under the Human Capital and Mobility Contract No. CHRX-CT93-0338.

[1] M. D. Perry and G. Mourou, Science **264**, 917 (1994).
[2] G. Mourou and D. Umstadter, Phys. Fluids B **4**, 2315 (1992).
[3] J. C. Gauthier, in *Laser Interaction with Matter*, edited by S. Rose, IOP Conf. Proc. No. 140 (Institute of Physics and Physical Society, Bristol, 1994), p. 1.
[4] P. Gibbon and E. Förster, Plasma Phys. Controlled Fusion **38**, 769 (1996).
[5] J. F. Pelletier, M. Chaker, and J. C. Kieffer, Opt. Lett. **21**, 1040 (1996).
[6] J. F. Pelletier, M. Chaker, and J. C. Kieffer, Appl. Phys. Lett. **69**, 2172 (1996).
[7] J. Workman, A. Maksimchuk, X. Liu, U. Ellenberger, J. S. Coe, X. -Y. Chien, and D. Umstadter, J. Opt. Soc. Am. B **13**, 125 (1996).
[8] J. C. Kieffer, M. Chaker, J. P. Matte, H. Pépin, C. Y. Côté, Y. Beaudoin, C. Y. Chien, S. Coe, G. Mourou, and O. Peyrusse, Phys. Fluids B **5**, 2676 (1993).
[9] A. Rousse, P. Audebert, J. P. Geindre, F. Falliès, J. -C. Gauthier, A. Mysyrowicz, G. Grillon, and A. Antonetti, Phys. Rev. E **50**, 2200 (1994).
[10] J. C. Kieffer, Z. Jiang, A. Ikhlef, and C. Y. Côté, J. Opt. Soc. Am. B **13**, 132 (1996).
[11] J. D. Kmetec, IEEE J. Quantum Electron. **28**, 2382 (1992).
[12] A. Rousse, P. Audebert, J. P. Geindre, F. Falliès, J. C. Gauthier, A. Mysyrowicz, A. Dos Santos, G. Grillon, and A. Antonetti, J. Phys. B **27**, L697 (1994).
[13] F. Ráksi, K. R. Wilson, Z. Jiang, A. Ikhlef, C. Y. Côté, and J. C. Kieffer, J. Chem. Phys. **104**, 6066 (1996).
[14] C. P. J. Barty, C. L. Gordon III, B. E. Lemoff, C. Rose-Petruck, F. Ráksi, P. M. Bell, K. R. Wilson, V. V. Yakovlev, K. Yamakawa, and G. Y. Yin, in *Applications of Laser Plasma Radiation II*, edited by M. C. Richardson and G. Kirala, Proceedings of SPIE—The International Society for Optical Engineering No. 2523 (SPIE, Bellingham, WA, 1995), p. 286.
[15] J. Nilsen, J. C. Moreno, L. B. Da Silva, and T. W. Barbee, Jr., in *X-ray Lasers 96*, edited by S. Svanberg and C. G. Wahl-

ström, IOP Conf. Proc. No. 151 (Institute of Physics and Physical Society, London, 1996), pp. 240–246.
[16] M. Berglund, L. Rymell, and H. M. Hertz, Appl. Phys. Lett. **69**, 1683 (1996).
[17] J. A. Cobble, G. T. Schappert, L. A. Jones, A. J. Taylor, G. A. Kyrala, and R. D. Fulton, J. Appl. Phys. **69**, 3369 (1991).
[18] O. Willi, G. Kiehn, J. Edwards, V. Barrow, R. A. Smith, J. Wark, and E. Turcu, Europhys. Lett. **10**, 141 (1989).
[19] P. Audebert, J. P. Geindre, and J. C. Gauthier, in *Atomic Processes in Plasmas*, edited by E. S. Marmar and J. L. Terry, AIP Conf. Proc. 257 (AIP, New York, 1991), p. 58.
[20] U. Teubner, G. Kühnle and F. P. Schäfer, Appl. Phys. B: Photophys. Laser Chem. **54**, 493 (1992).
[21] W. Theobald, C. Wülker, J. Jasny, S. Szatmáry, F. P. Schäfer, and J. S. Bakos, Phys. Rev. E **49**, R4799 (1994).
[22] H. Ahn, H. Nakano, T. Nishikawa, and N. Uesugi, Jpn. J. Appl. Phys., Part 2 **35**, L154 (1996).
[23] J. F. Pelletier, Ph.D. thesis, University of Montreal, 1996.
[24] H. C. Kapteyn, M. M. Murnane, A. Szoke, and R. W. Falcone, Opt. Lett. **16**, 490 (1991).
[25] D. M. Gold, Opt. Lett. **19**, 2006 (1994).
[26] V. L. Ginzburg, *The Propagation of EM Waves in Plasmas* (Pergamon, New York, 1970), Chap. 2, p. 100; W. L. Kruer, *The Physics of Laser Plasma Interactions* (Addison-Wesley, Redwood City, CA, 1988).
[27] W. Rozmus and V. T. Tikonchuk, Phys. Rev. A **42**, 7401 (1990).
[28] R. Fedosejevs, R. Ottmann, R. Sigel, G. Kühnle, S. Szatmari, and F. P. Schäfer, Appl. Phys. B: Photophys. Laser Chem. **50**, 79 (1990); Phys. Rev. Lett. **64**, 1250 (1990).
[29] T. -Y. Brian Yang, W. L. Kruer, A. B. Langdon, and T. W. Johnston, Phys. Plasmas **3**, 2702 (1996).
[30] F. Brunel, Phys. Rev. Lett. **59**, 52 (1987); Phys. Fluids **31**, 2714 (1988).
[31] G. Bonnaud, P. Gibbon, J. Kindel, and E. Williams, Laser Part. Beams **9**, 339 (1991).
[32] J. C. Kieffer, J. P. Matte, S. Bélair, M. Chaker, P. Audebert, H. Pépin, P. Maine, D. Strickland, P. Bado, and G. Mourou, IEEE J. Quantum Electron. **25**, 2640 (1989).
[33] R. Sauerbrey, B. van Wonterghem, J. Bergmann, U. Teubner, and F. P. Schäfer, in *OSA Proceedings on Shortwavelength V: Physics with Intense Laser Pulses*, edited by M. D. Perry and P. B. Corkum (Optical Society of America, Washington, DC, 1993), Vol. 17, p. 177–182.
[34] H. M. Milchberg and R. R. Freeman, J. Opt. Soc. Am. B **6**, 1351 (1989).
[35] H. M. Milchberg, R. R. Freeman, S. C. Davey, and R. M. More, Phys. Rev. Lett. **61**, 2364 (1988).
[36] D. F. Price, R. M. More, R. S. Walling, G. Guethlein, R. L. Shepherd, R. E. Stewart, and W. E. White, Phys. Rev. Lett. **75**, 252 (1995).
[37] J. -C. Gauthier, J. P. Geindre, P. Audebert, S. Bastiani, C. Quoix, G. Grillon, A. Mysyrowicz, A. Antonetti, and R. C. Mancini, Phys. Plasmas **4**, 1811 (1997).
[38] P. Gibbon, Phys. Rev. Lett. **73**, 664 (1994).
[39] D. D. Meyerhofer, H. Chen, J. A. Delettrez, B. Soom, S. Uchida, and B. Yaakobi, Phys. Fluids B **5**, 2584 (1993).
[40] P. Fews, P. A. Norreys, F. N. Beg, A. R. Bell, A. E. Dangor, C. N. Danson, P. Lee, and S. J. Rose, Phys. Rev. Lett. **73**, 1801 (1994).
[41] G. Guethlein, M. E. Foord, and D. Price, Phys. Rev. Lett. **77**, 1055 (1996).
[42] H. Hamster, A. Sullivan, S. Gordon, W. White, and R. W. Falcone, Phys. Rev. Lett. **71**, 2725 (1993).
[43] C. Rousseaux, F. Amiranoff, C. Labaune, and G. Mathieussent, Phys. Fluids B **4**, 2589 (1992).
[44] G. Malka and J. L. Miquel, Phys. Rev. Lett. **77**, 75 (1996).
[45] G. Malka, E. Lefebvre, and J. L. Miquel, Phys. Rev. Lett. **78**, 3314 (1997).
[46] J. P. Geindre, P. Audebert, A. Rousse, F. Falliès, J. C. Gauthier, A. Mysyrowicz, A. Dos Santos, G. Hamoniaux, and A. Antonetti, Opt. Lett. **19**, 1997 (1994).
[47] L. Lepetit, G. Chériaux, and M. Joffre, J. Opt. Soc. Am. B **12**, 2467 (1995).
[48] C. W. Siders, S. P. Le Blanc, A. Babine, A. Stepanov, A. Sergueev, T. Tajima, and M. C. Downer, IEEE Trans. Plasma Sci. **24**, 301 (1996).
[49] P. Blanc, P. Audebert, F. Falliès, J. P. Geindre, J. C. Gauthier, A. Dos Santos, A. Mysyrowicz, and A. Antonetti, J. Opt. Soc. Am. B **13**, 118 (1996).
[50] C. Le Blanc, G. Grillon, J. P. Chambaret, A. Migus, and A. Antonetti, Opt. Lett. **18**, 140 (1993).
[51] A. Sullivan and W. E. White, Opt. Lett. **20**, 192 (1995).
[52] P. Gibbon and A. R. Bell, Phys. Rev. Lett. **68**, 1535 (1992).
[53] J. Delettrez (private communication).
[54] R. Lichters, J. Meyer-ter-Vehn, and A. Pukhov, Phys. Plasmas **3**, 3425 (1996).
[55] R. Lichters, Ph.D. thesis, Technical University München, 1997; Max-Planck Institut für Quantenoptik Report No. 219, 1997 (unpublished).
[56] U. Teubner, D. Altenbernd, P. Gibbon, E. Förster, A. Mysyrowicz, P. Audebert, J. P. Geindre, J. C. Gauthier, R. Lichters, and J. Meyer-ter-Vehn, Opt. Commun. (to be published).
[57] H. Ruhl and P. Mulser, Phys. Lett. A **205**, 388 (1995).
[58] H. Ruhl, J. Opt. Soc. Am. B **13**, 388 (1996).
[59] H. Ruhl, Phys. Plasmas **3**, 3129 (1996).
[60] H. J. Kull, Phys. Fluids **26**, 1881 (1983).
[61] U. Teubner, P. Gibbon, E. Förster, F. Falliès, P. Audebert, J. P. Geindre, and J. C. Gauthier, Phys. Plasmas **3**, 2679 (1996).
[62] K. Estabrook and W. L. Kruer, Phys. Fluids **26**, 1888 (1983).
[63] H. Maki and K. Niu, J. Phys. Soc. Jpn. **45**, 269 (1978).